Memory hierarchy for many-body localization: Emulating the thermodynamic limit

Alexander Nico-Katz,[1,*] Abolfazl Bayat [ORCID],[2,†] and Sougato Bose[1,‡]

[1]*Department of Physics and Astronomy, University College London, London WC1E 6BT, United Kingdom*
[2]*Institute of Fundamental and Frontier Sciences, University of Electronic Science and Technology of China, Chengdu 610051, China*

Local memory—the ability to extract information from a subsystem about its initial state—is a central feature of many-body localization. We introduce, investigate, and compare several information-theoretic quantifications of memory and discover a hierarchical relationship among them. We also find that while the Holevo quantity is the most complete quantifier of memory, vastly outperforming the imbalance, its decohered counterpart is significantly better at capturing the critical properties of the many-body localization transition at small system sizes. This motivates our suggestion that one can emulate the thermodynamic limit by artificially decohering otherwise quantum quantities. Applying this method to the von Neumann entropy results in critical exponents consistent with analytic predictions, a feature missing from similar small finite-size system treatments. In addition, the decohering process makes experiments significantly simpler by avoiding quantum state tomography.

I. INTRODUCTION

Many-body localization (MBL) in disordered systems has been the subject of varied theoretical and experimental studies [1–7] and its features are widely recognized: (i) strong ergodicity-breaking and eigenstate thermalization hypothesis violation in the MBL phase [8–10], (ii) a rich many-body localization phase transition (MBLT) across the entire spectrum with highly debated properties [11–20], and (iii) emergent integrability and associated local memory [3,21–24] which provides a lucrative testbed for applications in quantum computing. Most of these characteristic signatures of MBL have been placed on firm quantitative footings through the imbalance [25–30] and magnetization [11,13,31,32], entanglement entropies [26,31,33–36], spatial correlations [37,38], unfolded level statistics [11,13,34,39–41], and myriad others [27,37,42,43]. A key concept in MBL is the emergence of memory: the local retention of information about initial conditions. Memory is necessarily temporal and thus typically discussed through dynamical quantities such as the imbalance and steady states of local observables, or deduced from entanglement and correlation spreading [26,28,40,44–46]. However, these quantities suffer from a range of problems which curtail their use as true quantifiers of memory. In fact, a good quantifier of memory is expected to satisfy two criteria: (i) it should have an informational interpretation in terms of the number of bits and (ii) it should contain temporal corre-

lations. To satisfy these criteria, an informational framework and, in particular, the Holevo quantity—an upper bound on the amount of classical information which a quantum channel can bear—have recently been introduced in MBL systems [47]. A systematic investigation among memory quantifiers, in accordance with the above criteria, is missing; as is a comparison of their relationship to extant quantities, especially in the context of MBL. In such an investigation, two important questions can be asked. First, which memory quantifier preserves the most
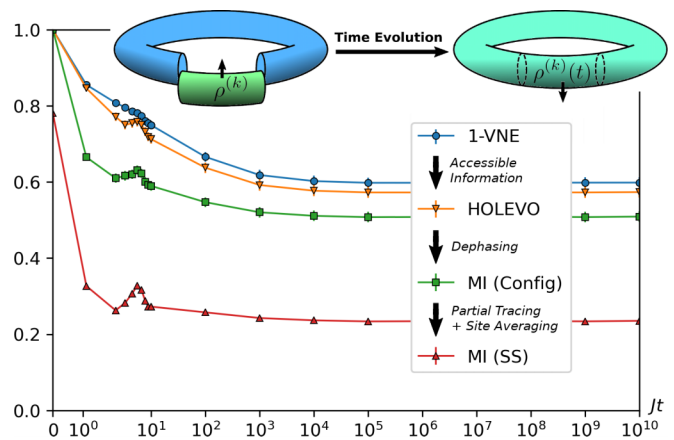

FIG. 1. Hierarchy of disorder-averaged informational quantities against time (normalized between 0 and 1) for disorder strength $h = 4$ in the middle of the MBLT. The schematic shows the action of a single channel realization on a single contiguous message state initialized in the state $\rho^{(k)} = |k\rangle\langle k|$. As each channel realization has a fixed disorder profile and environment state, we average over channels when constructing the quantities. The peak at $Jt \approx 8$ occurs when the information carried away from the message first interacts with itself, causing transient revival. Error bars are shown where visible. Results for both sides of the MBLT, $h = 0.1$ and $h = 16$, are given in Appendix A. All results are for $L = 16$ and $l = 4$.

*alex.nico-katz.15@ucl.ac.uk
†abolfazl.bayat@uestc.edu.cn
‡s.bose@ucl.ac.uk

information over time? Second, which memory quantifier best captures the properties of the ergodic-MBL transition? In particular, can one can establish a hierarchy on either of these grounds between different quantifiers and determine which best captures memory in MBL systems?

A central issue in MBL physics is the characterization of the transition point. Despite advancements in quantum simulators which allow for experimental attempts to access the transition [29,43,48–52] and theoretical breakthroughs, the nature of the transition is still highly debated [11–20]. Assuming the existence of a second-order phase transition, analytical results by Harris [53] and developments thereof [54,55] bound the critical exponent $\nu \geqslant 2$. Nevertheless, the limitation of exact numerics to small system sizes ($L \sim 20$) makes extracting thermodynamical behavior challenging; almost all small-scale numerical analyses—with few exceptions [42,56]—violate the Harris bound. Large phenomenological approaches—though blind to microscopic features of the system—have had markedly more success: achieving this bound [14,18,57–59]. Recent work even suggests that the transition may be of a Kosterlitz-Thouless type, and thus the Harris bound is inapplicable [19,20,60,61]. One may wonder whether a novel investigation of memory in small systems can reveal improved methods for analyzing the MBLT, bringing the small scale analyses in line with analytic and phenomenological results.

The paper is organized as follows. We begin by reviewing the model and unitary evolution in Sec. II. We then introduce, define, and discuss four different quantities in the informational framework, some of which bear resemblance to noninformational quantities already used in the context of MBL, in Sec. III. We compare these quantities with respect to two standards. First, in Sec. IV, which best captures memory in terms of the amount of information—in bits—retained over time; an analysis which reveals a strict hierarchy of memory quantifiers. Second, in Sec. V, which best captures critical behavior across the MBL transition in terms of minimizing the violation of the Harris bound [53–55]. This analysis reveals the insight that by artificially decohering a subsystem one can consistently reduce the amount by which the Harris bound is violated—in some cases even yielding results *consistent* with it. We discuss this finding in Sec. VI and suggest that this is due to the fact that artificially decohering a subsystem better emulates behavior at the thermodynamic limit, which we motivate with some preliminary results.

II. MODEL

We consider a system of l spin-1/2 particles which encode pure separable messages of the form $|k\rangle = |k_1, k_2, \ldots, k_l\rangle$, where $k_1 k_2 \ldots k_l$ is a binary representation of k, and where each $k_i \in \{0, 1\}$ is encoded in the physical system by spin up $|\uparrow\rangle$ and spin down $|\downarrow\rangle$ states, respectively. The index k runs over all 2^l configurations and thus $\{|k\rangle\}$ forms a complete orthonormal basis for the system, which we call the "message register." Note that, for the rest of this paper, we only consider contiguous message registers. Each message $|k\rangle$ is inserted into the message register with probability p_k. In this paper, we consider equiprobable messages, namely, $p_k = 1/2^l$. The message register is then embedded in a random environment

$|E\rangle$ of size $L - l$ (i.e., the total system size is L) which is initialized in a random product state of up and down spins. Thus, the initial state of the entire system is described by $|k\rangle\langle k| \otimes |E\rangle\langle E|$. The interactions between the particles are explained by the periodic Heisenberg Hamiltonian with random fields,

$$H = J \sum_{j=1}^{L} S_j \cdot S_{j+1} + \sum_{j=1}^{L} h_j S_j^z, \tag{1}$$

where J is the exchange coupling, $S_j = (S_j^x, S_j^y, S_j^z)$ is the vector of spin operators at site j, and the h_i's are random fields drawn uniformly in the interval $[-h, +h]$, with h characterizing the disorder strength. This model has been used extensively in MBL literature and is expected to localize for $h > h_c \gtrsim 3.7$ [15,61]. The quantum state of the message register at any time t, defined as $\rho^{(k)}(t)$, is given by the unitary evolution of the entire system and the partial tracing out of the environmental degrees of freedom:

$$\rho^{(k)}(t) = \mathrm{Tr}_E[e^{-iHt}(|k\rangle\langle k| \otimes |E\rangle\langle E|)e^{iHt}].$$

This procedure is shown in the schematic of Fig. 1. The goal is to quantify how much information—in bits—can be extracted locally from the message register at time t about its initial state. This temporal correlation between the past and the future is, essentially, "memory."

III. INFORMATIONAL QUANTITIES

We consider four quantities: (i) the von Neumann entropy, which has seen consistent use in MBL; (ii) the Holevo quantity; (iii) the classical single-site mutual information (SSMI) which is closely related to the widely used imbalance quantity; and (iv) the classical configurational mutual information (CMI), which has not been studied in the context of MBL. The last three are all true memory quantifiers in the sense that a memory quantifier is a quantity which (i) temporally correlates the initial and final states of a subsystem, and (ii) has a bitwise interpretation. Memory quantifiers can have various advantages over each other such as being optimal over measurement bases or experimentally tractable [47]. Whilst the schematic of Fig. 1 shows the effect of a single channel realization, each of these four quantities is averaged over 500–1000 realizations of the channel—the random fields and environment states—in a process we denote by $\langle \cdot \rangle$. For a summary of all quantities, see Table I.

In the following, we provide quantitative definitions for, and intuitive explanations of, these quantities. We emphasize that, though we have made an explicit choice of equiprobable messages such that the initial distribution is uniform, $p_k = 1/2^l$, these definitions generalize to any choice of p_k.

We define the normalized von Neumann entropy of the message register as

$$\overline{S(t)} = \frac{1}{l}\left\langle \sum_k p_k S[\rho^{(k)}(t)] \right\rangle, \tag{2}$$

where $S(\rho) = -\mathrm{Tr}\rho \log_2 \rho$. One may be motivated to suggest that the more mixed the subsystem $\rho^{(k)}(t)$ is on average, the less information has been retained within said subsystem, and

TABLE I. Summary of the four informational quantities discussed in this paper, whether they hold the status of a valid memory quantifier based on the criteria laid out in this paper and Ref. [47], and what measurements need to be made to construct the quantity.

Quantity	Memory quantifier	Measurements	Definition
Modified von Neumann entropy	No	Full state tomography	Eq. (2)
Holevo quantity	Yes	Full state tomography	Eq. (3)
Configurational mutual information (CMI)	Yes	Global measurements	Eq. (7)
Single-site mutual information (SSMI)	Yes	Local measurements	Eq. (5)

as such $1 - \overline{S(t)}$ is a quantifier of memory. However, this quantity contains no *accessible* informational content: in fact, whilst $\overline{S(t)}$ quantifies the average *instantaneous* mixedness of the states $\rho^{(k)}(t)$, it does so without regard for how well they bear information from the past or into the future. Consider, for instance, a channel which sends all initial states $\{|k\rangle\}$ to the single pure state $|0\rangle$. Clearly this channel is entirely useless for transmitting information, but $1 - \overline{S(t)}$ still saturates to unity. As such $1 - \overline{S(t)}$ is unsuitable as a memory quantifier. However, as we see in the following, it upper bounds all other true memory quantifiers and is widely used in MBL literature, and so serves as a useful benchmark.

The Holevo quantity [62,63] is a measure of the accessible classical information which can be accessed via optimal measurements on an ensemble of quantum states. Intuitively it can be understood as the maximum classical capacity of a quantum channel [64]. In Ref. [47] it has been proposed as a quantification of memory in MBL systems. For our setup, the normalized average Holevo quantity is defined as

$$\overline{C(t)} = \frac{1}{l}\left\langle S\left(\sum_k p_k \rho^{(k)}(t)\right) - \sum_k p_k S[\rho^{(k)}(t)]\right\rangle, \quad (3)$$

where the two message averages temporally connect the initial distribution encoded in the p_k's with the final distribution encoded in the mixed state of the message register $\rho^{(k)}(t)$—the essential feature of memory. We can intuit the Holevo quantity as constructed in Eq. (3) as a correction to $1 - \overline{S(t)}$ which accounts for whether or not the ensemble $\{\rho^{(k)}(t)\}$ actually bears information over time. Consider again the channel which sends all messages to $|k\rangle \rightarrow |0\rangle$; the first term in Eq. (3) accounts for this and causes $\overline{C(t)}$ to saturate to zero. Thus, whilst $1 - \overline{S(t)}$ upper bounds all quantities, $C(t)$ upper bounds the actual amount of *accessible* information contained in the system over time [65].

Experimentally, it is most convenient to measure local quantities in a single measurement basis, e.g., the computational basis. The joint probability that a site j in the message $|k\rangle$ is initialized in the state $\sigma \in \{0, 1\}$ and then measured at time t in the state $\sigma' \in \{0, 1\}$ is given by

$$p_{k,j}(\sigma, \sigma', t) = \text{tr}\big[P_j^{\sigma}|k\rangle\langle k|\big]\text{tr}\big[P_j^{\sigma'}\rho^{(k)}(t)\big], \quad (4)$$

where $P_j^{\sigma} = |\sigma_j\rangle\langle\sigma_j|$ is the projection operator at site j. These probabilities, when summed over all sites and states σ and σ' using appropriate phases and rescaled, are identical to the imbalance—a quantity which has been extensively utilized in MBL theory and experiment (see, for example, Refs. [25–30]) as a naïve measure of memory. To briefly summarize: the imbalance $\mathcal{I}$ is a sum over single-site autocorrelation functions in a fixed basis; e.g., for spinless fermions (the context in

which much of the work on the imbalance takes place) $\mathcal{I} = \sum_j \langle\Psi|n_j(0)n_j(t)|\Psi\rangle$, where $n_j(t)$ is the Heisenberg form of the number operator for site j at time t and where $|\Psi\rangle$ is the initial state of the system. In the ergodic regime, $\mathcal{I}$ fluctuates around zero, while in the MBL regime it fluctuates around a finite nonzero value. We can clearly see, in the case that $|\Psi\rangle$ is an eigenstate of each local number operator at $t = 0$, that we can rewrite each term in $\mathcal{I}$ in a form similar to that of Eq. (4). In essence, Eq. (4) is an information-theoretic version of the kind of measurements that are used to construct the imbalance. We then define the average SSMI as mutual information in terms of the $p_{k,j}(\sigma, \sigma', t)$:

$$\overline{I_s(t)} = \left\langle \sum_{k,\sigma,\sigma'} p_k \tilde{p}_k(\sigma, \sigma', t) \log_2 \frac{\tilde{p}_k(\sigma, \sigma', t)}{\tilde{p}_{k,\Sigma}(\sigma, t)\tilde{p}_{k,\Sigma'}(\sigma', t)} \right\rangle, \quad (5)$$

where $\tilde{p}_k(\sigma, \sigma', t) = \sum_j p_{k,j}(\sigma, \sigma', t)/l$ and where $p_{k,\Sigma(\Sigma')}[\sigma(\sigma'), t] = \sum_{\sigma'(\sigma)} \tilde{p}_k(\sigma, \sigma', t)$ are the marginal distributions of our site-averaged initial and final spin state variables, respectively. Thus, the SSMI is a natural information-theoretic extension of the imbalance in the sense that it is the information that can be extracted from the subsystem $\rho^{(k)}(t)$ about its initial configuration using *only* the measurements taken when computing the imbalance, namely, single-site measurements in a fixed basis.

One can extend the above idea to the whole message register, taking measurements in the basis of the message states $\{|k\rangle\}$. In this case, the outcome of the measurements is one of the 2^l spin configurations. The joint probability $p(k, k', t)$ of sending the state $|k\rangle$ and measuring the state $|k\rangle$ at time t is given by

$$p(k, k', t) = p_k\langle k'|\rho^{(k)}(t)|k'\rangle. \quad (6)$$

We then define the normalized CMI for this joint probability as

$$\overline{I_c(t)} = \frac{1}{l}\left\langle \sum_{kk'} p(k, k', t) \log_2 \frac{p(k, k', t)}{p_K(k, t)p_{K'}(k', t)} \right\rangle, \quad (7)$$

where $p_{K(K')}[k(k'), t] = \sum_{k'(k)} p(k, k', t)$ are the marginal distributions of our initial and final state variables, respectively. Importantly, as shown in Appendix A, this construction is exactly the Holevo quantity of Eq. (3) in the limit of a fully decohered message register, in which $\rho^{(k)}(t)$ is replaced by a decohered density matrix $\rho_D^{(k)}(t)$ with all off-diagonal elements set to zero:

$$\rho^{(k)}(t) \rightarrow \rho_D^{(k)}(t) = \text{diag}\big[\rho_{11}^{(k)}(t), \rho_{22}^{(k)}(t), \ldots, \rho_{2^l 2^l}^{(k)}(t)\big]. \quad (8)$$

In this sense, we can understand $\overline{I_c(t)}$ as direct counterpart to the quantity $\overline{C(t)}$ after all output states have been passed

through the fully decohering channel of Eq. (8). We emphasize here that the decohering process occurs only on the message register *after* full unitary evolution up to time t. Thus, while it destroys all coherence within the message register at the time of measurement, it does not preclude the buildup of long-range coherences during the unitary evolution of the full system.

Finally, we draw attention to an important feature of the memory quantifiers in that they are each constructed using different kinds of measurements. The Holevo quantity requires full tomography of the subsystem, the CMI requires measurements in a fixed global basis on the subsystem, and the SSMI requires the same measurements as the imbalance, namely, local measurements in a fixed basis. As such, these quantities give us a useful quantification of the maximum amount of information that can be extracted from a subsystem given the measurements accessible to the experimenter—a crucial point when considering the potential of MBL systems in quantum computational settings. We summarize all quantities, the measurements required to construct them, and their status as memory quantifiers in Table I.

IV. COMPARISON OF MEMORY QUANTIFIERS

The above quantities, except the normalized von Neumann entropy $\overline{S(t)}$, establish temporal correlations between the distribution of messages inserted into the message register at $t = 0$ and their final states at time t. In addition, all these quantities are defined such that they are bounded between 0 and 1. Thus the SSMI, CMI, and Holevo quantity are directly comparable as memory quantifiers, and each capture local memory differently depending on the measurements available. The von Neumann entropy upper bounds all quantities and serves as a useful benchmark. We compare these quantities with respect to two standards: (i) which better captures local memory in terms of the number of bits of information preserved in the subsystem over time, and (ii) which better captures the critical properties of system Eq. (1) as we scan h across the MBLT in terms of how strongly each quantity violates the Harris bound. The latter case is discussed in the scaling analysis later in this paper, but the former question: which quantity is a better memory quantifier?, is quickly addressed here.

In Fig. 1, we plot these four quantities as a function of time for a system of $L = 16$, $l = 4$, and $h/J = 4$. Exact diagonalization and subsequent time evolution were carried out using modifications of the QUIMB package [66]. One can clearly see that these quantities form a strict hierarchy at all times. Indeed, we conjecture that the four quantities obey the following inequality for all choices of L, l, and h:

$$1 - \overline{S(t)} \geqslant \overline{C(t)} \geqslant \overline{I_c(t)} \geqslant \overline{I_s(t)}. \tag{9}$$

In Appendix A, we strictly prove that $1 - \overline{S(t)} \geqslant \overline{C(t)} \geqslant \overline{I_c(t)}$. The last part of the inequality of Eq. (9), namely, the CMI upper bounding the SSMI has been extensively verified through numerical simulation and is intuitively sensible: dephasing and tracing out parts of a system should not increase the information we can glean from it. Indeed all the inequalities above have intuitive origins in quantum information: as discussed in Sec. IV, the Holevo quantity is a correction to $1 - \overline{S(t)}$ that specifically addresses whether or not information

in the subsystem is accessible given optimal measurements. The CMI is simply the Holevo quantity after all final message states have been passed through the fully dephasing channel in Eq. (8), and by the monotonicity of the Holevo quantity under such a channel, the inequality $\overline{C(t)} \geqslant \overline{I_c(t)}$ is evident. This is illustrated in the legend of Fig. 1, showing the hierarchy and the intuitive informational reasons for its existence. Thus, from a quantum informational perspective, the hierarchy of Eq. (9) is unsurprising. However, exploiting this informational framework and placing the hierarchy in the context of MBL reveals an important consequence: the imbalance—widely used as a quantifier of local memory in MBL—via its informational counterpart $\overline{I_s(t)}$, drastically underestimates memory in MBL systems. In the worst cases (see Fig. 1), the use of $\overline{I_s(t)}$ erases almost two-thirds of the accessible information according to the Holevo quantity.

A final feature of Fig. 1 is that all the four quantities have readily reached a steady state within very small error bars, even in the midst of the MBLT. This allows us to define time-independent steady-state quantities:

$$\overline{O}^{(\text{ss})} = \lim_{t \to \infty} \overline{O(t)} \approx \overline{O(T)}, \tag{10}$$

where O can be any of our four quantities, namely, $\overline{S(t)}$, $\overline{C(t)}$, $\overline{I_c(t)}$, and $\overline{I_s(t)}$, and where we take exponential times of $T = 10^{10} Jt$ for all results. These steady states can be used for investigating the scaling analysis across the MBL transition point, which is the subject of Sec. V of this paper.

V. SCALING ANALYSIS

In our setup, we deal with two explicit lengths, namely, message length l and the total system size L. Inspired by Refs. [15,55], it is expected that the steady-state values follow a finite-size anstaz of the form

$$\overline{O}^{(\text{ss})} = L^{-\zeta/\nu} f[l/L, L^{1/\nu}(h - h_c)], \tag{11}$$

where h_c is the critical point, ν and ζ are critical exponents, and $f(\cdot, \cdot)$ is an unspecified function. By fixing the ratio of $l/L = 1/3$, we plot $\overline{O}^{(\text{ss})}$ as a function of h for various system sizes in Figs. 2(a)–2(d) for all the four quantities, respectively. As is clear from the figure, all four quantities show a crossover between the curves of different sizes. The existence of this crossover indicates that $\zeta = 0$ and determines the critical value h_c for each quantity. Interestingly, the critical point h_c determined by the SSMI is far lower than the ones deduced from the other three quantities.

A more elaborate scaling analysis [36,67], based on the principle of data collapse, using the ansatz of Eq. (11) allows us to more precisely determine h_c, ζ, and ν. Indeed, our results with variable ζ (not shown) confirms that $\zeta \approx 0$ for all quantities. Hence, we set $\zeta = 0$ for the rest of the article. Respective data collapses for each quantity are shown in the insets of Figs. 2(a)–2(d), each yielding slightly different optimal values for ν and h_c. The optimal values for h_c and ν are depicted in Fig. 3(a). Similar to many previous studies: small system sizes lead to systematic underestimation of the critical value ν, bounded analytically for this system by $\nu \geqslant 2$ [53–55]. Additional scaling results are given in Appendix B.
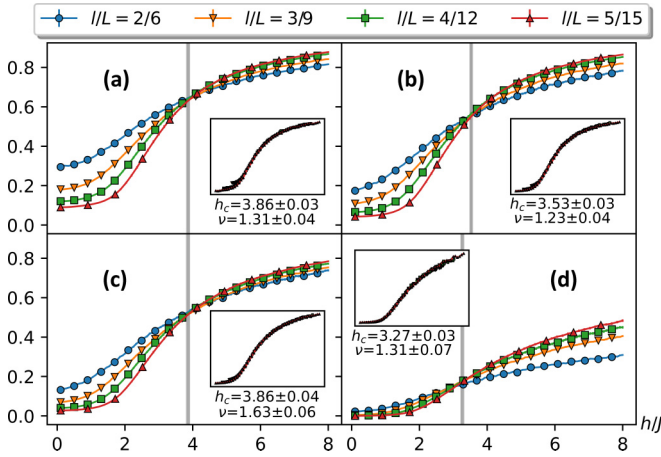
FIG. 2. Disorder-averaged steady-state values of (normalized) informational quantities as a function of disorder strength. The message-to-system size ratio for all panels is $l/L = 1/3$. The panels show (a) von Neumann entropy, (b) Holevo quantity, (c) CMI, and (d) SSMI. Insets show the corresponding data collapse for the three largest systems. Every fifth point is marked for legibility, and error bars are shown where visible.

The von Neumann entropy $\nu = 1.31 \pm 0.04$, the Holevo quantity $\nu = 1.23 \pm 0.04$, and the SSMI $\nu = 1.31 \pm 0.07$ all violate the Harris bound to a similar extent. Unexpectedly, all three of these quantities are outperformed in terms of the Harris-bound violation by the CMI which attains a critical exponent of $\nu = 1.63 \pm 0.06$, a remarkably high value for such small system sizes. In this sense we can state that the CMI may capture less information than the Holevo quantity (see the hierarchy of Fig. 1), but it does better capture the MBLT in the sense that it violates the Harris bound to a lesser extent. Finally, the SSMI performs badly both as the worst quantity with which to capture retained information and as a quantity which violates the Harris bound to a much greater extent than the CMI. It also underestimates the critical h_c with respect to all other quantities. This indicates that the
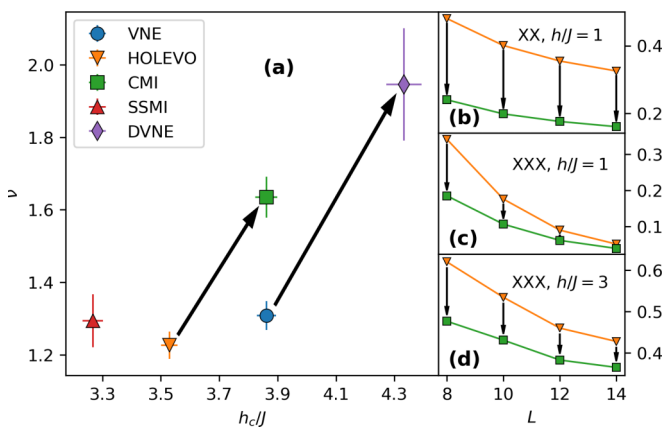
SSMI and, thus, the widely used imbalance are poor scaling quantities which cannot precisely capture properties of the MBLT. As such the SSMI and, by extension, the imbalance are not useful quantifiers of local memory in any arena other than situations where—due to the simple measurements they require—they are the only ones available.

VI. EMULATING THERMODYNAMIC BEHAVIOR

The significantly higher values of ν for the CMI may suggest that this quantifier better captures the behavior of Eq. (1) in the thermodynamic limit than the other quantities. Since the CMI is the decohered counterpart of the Holevo quantity, it indicates that throwing away the off-diagonal terms improves scaling results in terms of reducing the violation of the analytic bound $\nu > 2$. For small systems, where these off-diagonal quantum terms persist, we propose that it is beneficial to artificially set them to zero at the end of a simulation, or to only extract diagonal elements in experiment.

To further support this, we compute the decohered von Neumann entropy (DVNE) by decohering the message register $\rho \rightarrow \rho_D$ according to Eq. (8) in Eq. (2). This is essentially the Shannon entropy of diagonal elements in the computational basis and has been used sparsely in the context of MBL before [28,56,68]. The obtained critical values of h_c and ν are plotted in Fig. 3(a). The effect of artificial dephasing according to Eq. (8) is shown in Fig. 3 by the black arrows. Remarkably, the von Neumann entropy of artificially dephased quantum states yields a critical value $\nu = 1.95 \pm 0.15$ consistent with the Harris bound [53] and closer to large-system analyses of the MBLT. We see similar results in the additional scaling analyses shown in Appendix B.

We conjecture that this may be because artificially decohering the message subsystem imitates the kind of effects that occur in the thermodynamic limit. The decohering of a subsystem in the thermodynamic limit is a direct consequence of interactions, a consequence we investigate by comparing the steady-state Holevo quantity and its decohered counterpart, the CMI, directly in interacting and interactionless systems across the MBLT. In Fig. 3(b) we replace the Heisenberg (XXX) Hamiltonian of Eq. (1) with the interactionless (XX) Hamiltonian. Even for small disorder strength $h/J = 1$, the figure shows slight—if any—convergence between the Holevo quantity and the CMI as L increases. In Figs. 3(c)–3(d) we return to the Heisenberg Hamiltonian. On the small disorder $h/J = 1$ side of the MBLT shown in Fig. 3(c), the Holevo quantity and the CMI quickly converge as the system size increases. While, close to the transition point $h/J = 3$, we can see from Fig. 3(c) that the convergence as L increases is still clear, but slowed significantly. From this, we can deduce that the dephasing of the subsystem slows down near the MBL transition point and thus larger system sizes are required to emulate thermodynamic behavior. This explains why wholly quantum quantities may fail to capture the Harris bound $\nu \geqslant 2$ in small finite systems $L \sim 20$. Essentially, rather than completing this convergence by taking L to a sufficiently large value, our suggestion approximates it by artificially decohering the subsystem instead.

We note here that this procedure enforces a particular understanding of the nature of the MBL state in the

FIG. 3. Panel (a) shows the optimal critical values h_c and the exponents ν for all memory quantifiers and the DVNE. Panels (b)–(d) compare the Holevo quantity and its decohered counterpart, the CMI, in the XX and Heisenberg (XXX) models. Artificial dephasing is indicated by the arrows.

thermodynamic limit: as a product of subsystems which eventually dephase. As such we can only conjecture that this procedure emulates the thermodynamic limit, though we support that conjecture with some preliminary evidence [see Figs. 3(b)–3(d)] and argument. What we can state definitively is that this procedure considerably reduces the extent to which the analytic Harris bound is violated in small systems [see Fig. 3(a)], which in turn is evidence that such an enforcement is plausible.

VII. CONCLUSIONS

We introduce several quantities for quantification of memory in MBL systems and establish a systematic hierarchical order among them. Our findings show that the Holevo quantity represents the best quantifier of memory in terms of number of bits of information retained over time and that the informational version of the widely used imbalance performs the worst. Furthermore when characterizing the MBL transition using these memory quantifiers we find that, though the Holevo quantity is the best quantifier of memory, the CMI—its decohered counterpart—best captures the critical properties of the MBLT. Motivated by this, we compared the von Neumann entropy of a small subsystem to its decohered variant and discovered that it too outperforms its quantum, coherent, counterpart; yielding a critical exponent consistent with the Harris bound. Our conclusion is that finite-size effects can be mitigated just by deliberately decohering the final state of the message register. This has huge theoretical and experimental advantages: in theory one can drastically improve small-system scaling results and may even be able to emulate the thermodynamic limit by deliberately throwing away information, and in experiment one only needs to measure the diagonal elements of the reduced density matrix instead of using extremely demanding state tomography.

ACKNOWLEDGMENTS

APPENDIX A: THE MEMORY HIERARCHY

Here we derive the first two inequalities in the memory hierarchy $1 - \overline{S(t)} \geqslant \overline{C(t)} \geqslant \overline{I_c(t)} \geqslant \overline{I_s(t)}$ discussed in the main text. We also discuss a few technical nuances and justifications for our construction of $\overline{I_s(t)}$. We derive the inequalities for a single ensemble of initial probabilities $\{p_k\}$ and final quantum states $\{\rho^{(k)}(t)\}$. Clearly, if it holds for each individual ensemble, it holds for the disorder and environment (channel) average over those ensembles as well. We denote each quantity for a single channel realization using the index r, e.g., $\overline{S(t)} = \frac{1}{N_r} \sum_r S^r(t)$, where N_r is the number of samples. We suppress this index on the density operators $\rho^{(k)}(t)$ themselves for readability. Thus, the hierarchy we derive here for the

largest three quantities is *stricter* than that stated in the main text: $1 - S^r(t) \geqslant C^r(t) \geqslant I_c^r(t)$.

The first inequality $1 - S^r(t) \geqslant C^r(t)$ trivially follows from our definition of the normalized von Neumann entropy over the ensemble:

$$S^r(t) = \frac{1}{l} \sum_k p_k S[\rho^{(k)}(t)], \tag{A1}$$

where $S(\rho) = -\mathrm{Tr}\rho \log_2 \rho$, and our definition of the Holevo quantity:

$$C^r(t) = \frac{1}{l} S\left(\sum_k p_k \rho^{(k)}(t)\right) - \frac{1}{l} \sum_k p_k S[\rho^{(k)}(t)]. \tag{A2}$$

By taking the difference of the two quantities $\Delta_{SC}^r(t)$ and noting that the second term in the Holevo quantity is just $S^r(t)$, it follows that

$$\Delta_{SC}^r(t) = 1 - S^r(t) - C^r(t) = 1 - \frac{1}{l} S\left(\sum_k p_k \rho^{(k)}(t)\right), \tag{A3}$$

where the second term clearly saturates to its maximum value of unity as $\sum_k p_k \rho^{(k)}(t)$ approaches the identity. As such $\Delta_{SC}^r(t) \geqslant 0$ and the inequality $1 - S^r(t) \geqslant C^r(t)$ follows. This gives us an intuitive understanding of the Holevo quantity as a modification to $1 - S^r(t)$, accounting for how much information is *accessible* at time t rather than how useful the $\rho^{(k)}(t)$'s are as an instantaneous alphabet.

The derivation of the second inequality is slightly more involved, first requiring us to show that the CMI $I_c^r(t)$ is just a fully decohered version of the Holevo quantity $C^r(t)$. We carry out the derivation in the computational basis, but in principle any suitable basis can be used instead. In the computational basis, and given the $\{p_k\}$ *a priori*, the joint probability $p(k, k', t)$ of sending the state k and measuring the state k' at time t is determined entirely by the diagonal elements of $\rho^{(k)}(t)$:

$$p(k, k', t) = p_k \rho_{k'k'}^{(k)}(t). \tag{A4}$$

We then compute the classical mutual information according to the well-known formula

$$I_c^r(t) = \frac{1}{l} \sum_{kk'} p(k, k', t) \log_2 \frac{p(k, k', t)}{\sum_s p(k, s, t) \sum_{s'} p(s', k', t)}, \tag{A5}$$

where the first marginal distribution $\sum_s p(k, s, t)$ resolves trivially to p_k by the unit-trace condition [see Eq. (A4)]. The second marginal distribution $\sum_{s'} p(s', k', t)$ involves all message states and is generally nontrivial. Evaluating the first marginal distribution, splitting up the logarithm, and canceling relevant terms yields the following:

$$I_c^r(t) = \frac{1}{l} \sum_{kk'} p_k \rho_{k'k'}^{(k)}(t) \log_2 \rho_{k'k'}^{(k)}(t)$$
$$- \frac{1}{l} \sum_{kk'} p_k \rho_{k'k'}^{(k)}(t) \log_2 \sum_{s'} p_{s'} \rho_{k'k'}^{(s')}(t). \tag{A6}$$

We note that, by constructing an operator with the $\rho_{k'k'}^{(k)}(t)$ as eigenvalues, the sums over k' can be replaced with appropriate
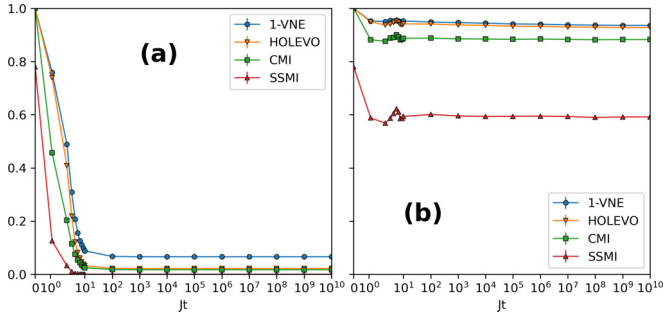
FIG. 4. Dynamics of the four informational quantities for $L = 16$ and $l = 4$ on extreme sides of the MBLT: (a) $h = 0.1$ and (b) $h = 16$. Results for the middle of the MBLT ($h = 4$) are given in the main text. In all cases, a strict hierarchy is seen, and the system convincingly relaxes to a steady state at exponential times.

traces and some terms will take the form of von Neumann entropies. A naturally suitable operator is the the fully decohered (in the computational basis) operator $\rho_D^{(k)}(t)$, defined as the leading diagonal of $\rho^{(k)}(t)$:

$$\rho^{(k)}(t) \rightarrow \rho_D^{(k)}(t) = \mathrm{diag}\big(\rho_{11}^{(k)}(t), \rho_{22}^{(k)}(t), \ldots, \rho_{2^l 2^l}^{(k)}(t)\big),$$
(A6)

which trivially has the $\rho_{k'k'}^{(k)}(t)$'s as eigenvalues. We can then recast $I_c^r(t)$ in terms of traces as follows:

$$I_c^r(t) = \frac{1}{l} \sum_k p_k \mathrm{Tr}\big[\rho_D^{(k)}(t) \log_2 \rho_D^{(k)}(t)\big]$$
$$- \frac{1}{l} \mathrm{Tr}\left[\left(\sum_k p_k \rho_D^{(k)}(t)\right) \log_2 \left(\sum_s p_s \rho_D^{(s)}(t)\right)\right],$$

which, when rewritten in terms of the von Neumann entropy $S(\rho) = -\mathrm{Tr}\rho \log_2 \rho$, yields the Holevo quantity over decohered states $\rho_D^{(k)}(t)$:

$$I_c^r(t) = \frac{1}{l} S\left(\sum_k p_k \rho_D^{(k)}(t)\right) - \frac{1}{l} \sum_k p_k S\big[\rho_D^{(k)}(t)\big], \quad \text{(A7)}$$

demonstrating, by analogy to Eq. (A2), that the configurational mutual information as we have constructed it is just the Holevo quantity in the full decoherence limit. Though we have chosen the computational basis for our derivation, any suitable (orthonormal) basis can be used. We can intuit that different choices of basis yield different diagonal elements in the $\rho_D^{(k)}(t)$'s, and act as effective modifications to the eigenvalues of all the $\rho^{(k)}(t)$'s at once. The Holevo quantity is "optimal" in the sense that it uses the true eigenvalues of the $\rho^{(k)}(t)$'s,
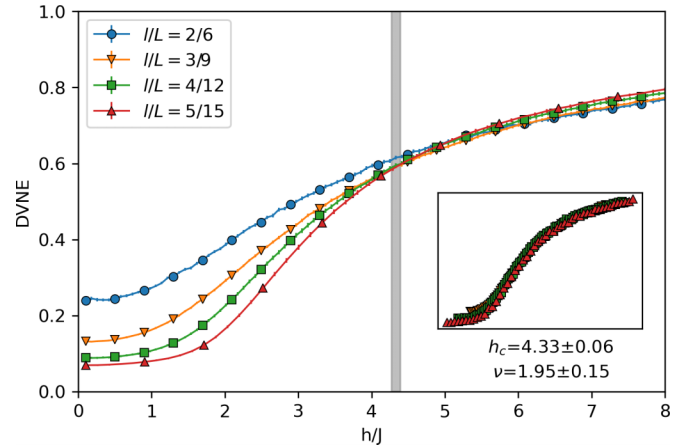

FIG. 5. Scaling of the DVNE discussed in the main text (message to system size ratio $l/L = 1/3$). Every fifth point is marked for readability, and error bars are shown where visible. The inset shows the corresponding data collapse of the largest three systems.

equivalent to performing measurements in the eigenbasis of each individual $\rho^{(k)}(t)$.

We now derive the second strict inequality $C^r(t) \geqslant I_c^r(t)$ by defining the difference of the two quantities:

$$l\Delta_{CI}^r(t) = lC^r(t) - lI_c^r(t),$$
(A8)

where we have multiplied by l to suppress the normalization constants and avoid notational clutter in the derivation to come. We then insert the Holevo quantity of Eq. (A2) and the dephased Holevo form of the CMI of Eq. (A7), and we fully expand the von Neumman entropies:

$$l\Delta_{CI}^r(t) = -\mathrm{Tr}\left[\left(\sum_k p_k \rho^{(k)}(t)\right) \log_2 \left(\sum_k p_k \rho^{(k)}(t)\right)\right]$$
$$+ \sum_k p_k \mathrm{Tr}\big[\rho^{(k)}(t) \log_2 \rho^{(k)}(t)\big]$$
$$+ \mathrm{Tr}\left[\left(\sum_k p_k \rho_D^{(k)}(t)\right) \log_2 \left(\sum_k p_k \rho_D^{(k)}(t)\right)\right]$$
$$- \sum_k p_k \mathrm{Tr}\big[\rho_D^{(k)}(t) \log_2 \rho_D^{(k)}(t)\big].$$

We now remark that the operators $\log_2 \rho_D^{(k)}(t)$ and $\log_2 \sum_k p_k \rho_D^{(k)}(t)$ are diagonal by definition; so any matrix multiplication between them and another operator will only involve the diagonal elements of both. Thus, all the $\rho_D^{(k)}(t)$ *outside* those logarithms can be replaced by the corresponding original operators $\rho^{(k)}(t)$. We perform this replacement, collect like terms, and manipulate $l\Delta_{CI}^r(t)$ into a revealing form:

$$l\Delta_{CI}^r(t) = -\mathrm{Tr}\left\{\left(\sum_k p_k \rho^{(k)}(t)\right)\left[\log_2 \left(\sum_k p_k \rho^{(k)}(t)\right) - \log_2 \left(\sum_k p_k \rho_D^{(k)}(t)\right)\right]\right\}$$
$$+ \sum_k p_k \mathrm{Tr}\big[\rho^{(k)}(t)\big(\log \rho^{(k)}(t) - \log \rho_D^{(k)}(t)\big)\big],$$
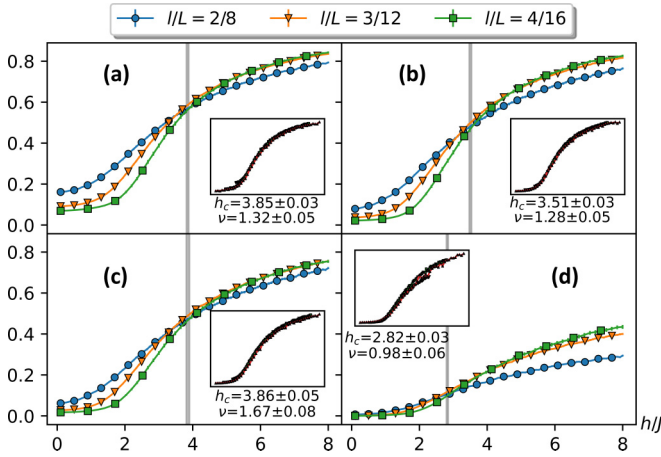
FIG. 6. Steady-state values of the four informational quantities, (a) von Neumann, (b) Holevo quantity, (c) CMI, and (d) SSMI, against disorder for the message to system ratio $l/L = 1/4$. Inserts show corresponding data collapses. Gray regions depict the extracted critical values and their errors.

FIG. 7. Extracted critical values and exponents for the memory quantifiers for the message to system size ratio $l/L = 1/4$. Black arrows show artificial decohering [see Eq (A6) and main text] which systematically increases the extracted critical values to be closer to large-scale phenomenological studies and analytic bounds. The DVNE is even consistent with the Harris bound $\nu = 1.98 \pm 0.17 \geqslant 2$.

in which both terms clearly take the form of quantum relative entropies $S(\rho||\sigma) = \text{Tr}[\rho(\log_2 \rho - \log_2 \sigma)]$. Explicitly, we can rewrite $\Delta_{CI}^r(t)$ as follows (reintroducing the normalization factor):

$$\Delta_{CI}^r(t) = -\frac{1}{l}S\left(\sum_k p_k \rho^{(k)}(t) \middle\| \sum_k p_k \rho_D^{(k)}(t)\right)$$
$$+ \frac{1}{l}\sum_k p_k S(\rho^{(k)}(t)||\rho_D^{(k)}(t)),$$

in which, by the joint convexity of the quantum relative entropy, the second term is greater than or equal to the first. As such, $\Delta_{CI}^r(t) \geqslant 0$ and the Holevo quantity upper bounds the CMI $C^r(t) \geqslant I_c^r(t)$. We can understand this in two highly intuitive ways: (i) the CMI is "suboptimal" with respect to the Holevo quantity in the sense that it uses a single, fixed, measurement basis, and (ii) decoherence and measurements cannot increase the information accessible in a system. Numerical results which clearly show this hierarchy in the middle of the many-body localization transition (MBLT) for $h = 4$ are given in the main text, whilst results on the extreme sides of the transition ($h = 0.1$ and $h = 16$) are shown in Fig. 4.

We conclude this section with a brief discussion of the single-site mutual information (SSMI) $\overline{I_s(t)}$ as defined in the main text. We intuit the final inequality $\overline{I_c(t)} \geqslant \overline{I_s(t)}$ in a similar fashion: the SSMI is constructed using repeated partial traces and projections on the systems used in the construction of the CMI. Such operations cannot increase the information in a system, and so we expect the CMI to systematically upper bound the SSMI. This has been convincingly verified numerically (see main text). Finally, in our definition of the SSMI in the main text, we average over individual sites and messages in an order that may appear arbitrary: taking the site average at the level of individual probabilities and the message average at the level of disorder/environment (channel) averaging. Our justifications follow four ideas.
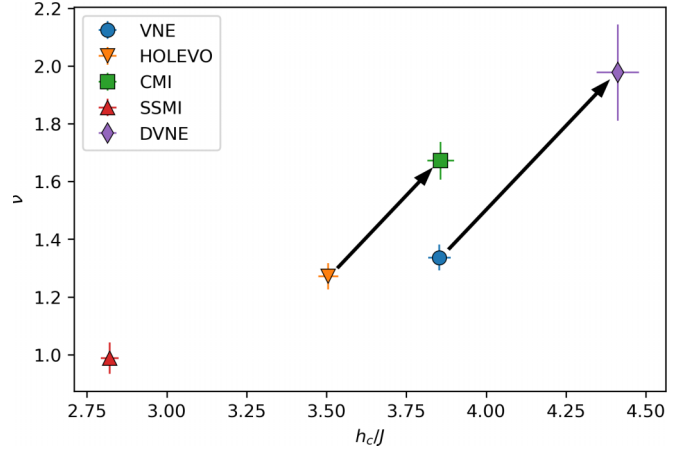
(i) An average must be taken, without averaging the protocol sends a single message with probability unity, and as such cannot bear information. This can be verified by inspection of the definition of $\overline{I_s(t)}$ in the main text.

(ii) For a given site, the rest of the message forms part of the environment.

(iii) We define the SSMI analogously to the conventional imbalance which averages over each site per realization.

(iv) Our results (not shown) for taking the combined order—with both site and message averaging at the level of individual probabilities—yield no scaling results and show an overall decrease in informational content with increasing system size; indicating that this decoding protocol is essentially useless.

APPENDIX B: ADDITIONAL SCALING RESULTS

In this section we provide, for completeness, additional results regarding the characterization of the MBLT. In the main text we discuss the decohered von Neumann entropy (DVNE), which is essentially a Shannon entropy of the diagonal elements of the density matrix in some given basis. The steady states and corresponding data collapse of the DVNE used in the main text (for $l/L = 1/3$) are given in Fig. 5. We can see that—with the exception of the two-site $l = 2$ and $L = 6$ case—the curves intersect. The critical value $h_c = 4.33 \pm 0.06$ and the exponent $\nu = 1.95 \pm 0.15$ were retrieved from the corresponding data collapse (inset of Fig. 5) of the largest three system sizes ($L = 9$, 12, and 15).

We also provide the identical analysis as given in the main text, but for the length ratio $l/L = 1/4$ instead. Due mostly to the fact that the numerical procedure by which the Holevo quantity is calculated scales with an additional factor of order $O(2^l)$, on top of the already $O(2^L)$ scaling of the underlying Hilbert space, this is limited by computational power to three curves: $L = 8$, 12, and 16. As

such the scalings may suffer from finite-size effects different from, and stronger than, those discussed in the main text and above. The steady states are shown in Fig. 6, and the corresponding critical values and exponents are shown in Fig. 7. Despite this, we can see that the decoherence procedure (black arrows) still systematically increases ν towards the results of analytics and large phenomenological analyses of the MBLT.

[1] P. W. Anderson, Absence of diffusion in certain random lattices, Phys. Rev. **109**, 1492 (1958).

[2] D. Basko, I. Aleiner, and B. Altshuler, Metal-insulator transition in a weakly interacting many-electron system with localized single-particle states, Ann. Phys. (Amsterdam, Neth.) **321**, 1126 (2006).

[3] J. Z. Imbrie, On many-body localization for quantum spin chains, J. Stat. Phys. **163**, 998 (2016).

[4] R. Nandkishore and D. A. Huse, Many-body localization and thermalization in quantum statistical mechanics, Annu. Rev. Condens. Matter Phys. **6**, 15 (2015).

[5] E. Altman and R. Vosk, Universal dynamics and renormalization in many-body-localized systems, Annu. Rev. Condens. Matter Phys. **6**, 383 (2015).

[6] F. Alet and N. Laflorencie, Many-body localization: An introduction and selected topics, C. R. Phys. **19**, 498 (2018).

[7] D. A. Abanin, E. Altman, I. Bloch, and M. Serbyn, Colloquium: Many-body localization, thermalization, and entanglement, Rev. Mod. Phys. **91**, 021001 (2019).

[8] J. M. Deutsch, Quantum statistical mechanics in a closed system, Phys. Rev. A **43**, 2046 (1991).

[9] M. Srednicki, Chaos and quantum thermalization, Phys. Rev. E **50**, 888 (1994).

[10] M. Rigol, V. Dunjko, and M. Olshanii, Thermalization and its mechanism for generic isolated quantum systems, Nature (London) **452**, 854 (2008).

[11] A. Pal and D. A. Huse, Many-body localization phase transition, Phys. Rev. B **82**, 174411 (2010).

[12] T. Grover, Certain general constraints on the many-body localization transition, arXiv:1405.1471

[13] D. J. Luitz, N. Laflorencie, and F. Alet, Many-body localization edge in the random-field Heisenberg chain, Phys. Rev. B **91**, 081103(R) (2015).

[14] A. C. Potter, R. Vasseur, and S. A. Parameswaran, Universal Properties of Many-Body Delocalization Transitions, Phys. Rev. X **5**, 031033 (2015).

[15] V. Khemani, S. P. Lim, D. N. Sheng, and D. A. Huse, Critical Properties of the Many-Body Localization Transition, Phys. Rev. X **7**, 021013 (2017).

[16] V. Khemani, D. N. Sheng, and D. A. Huse, Two Universality Classes for the Many-Body Localization Transition, Phys. Rev. Lett. **119**, 075702 (2017).

[17] T. Thiery, F. Huveneers, M. Müller, and W. De Roeck, Many-Body Delocalization as a Quantum Avalanche, Phys. Rev. Lett. **121**, 140601 (2018).

[18] A. Goremykina, R. Vasseur, and M. Serbyn, Analytically Solvable Renormalization Group for the Many-Body Localization Transition, Phys. Rev. Lett. **122**, 040601 (2019).

[19] P. T. Dumitrescu, A. Goremykina, S. A. Parameswaran, M. Serbyn, and R. Vasseur, Kosterlitz-Thouless scaling at many-body localization phase transitions, Phys. Rev. B **99**, 094205 (2019).

[20] A. Morningstar, D. A. Huse, and J. Z. Imbrie, Many-body localization near the critical point, Phys. Rev. B **102**, 125134 (2020).

[21] M. Serbyn, Z. Papić, and D. A. Abanin, Local Conservation Laws and the Structure of the Many-Body Localized States, Phys. Rev. Lett. **111**, 127201 (2013).

[22] D. A. Huse, R. Nandkishore, and V. Oganesyan, Phenomenology of fully many-body-localized systems, Phys. Rev. B **90**, 174202 (2014).

[23] V. Ros, M. Müller, and A. Scardicchio, Integrals of motion in the many-body localized phase, Nucl. Phys. B **891**, 420 (2015).

[24] A. Chandran, I. H. Kim, G. Vidal, and D. A. Abanin, Constructing local integrals of motion in the many-body localized phase, Phys. Rev. B **91**, 085425 (2015).

[25] M. Schreiber, S. S. Hodgman, P. Bordia, H. P. Lüschen, M. H. Fischer, R. Vosk, E. Altman, U. Schneider, and I. Bloch, Observation of many-body localization of interacting fermions in a quasirandom optical lattice, Science **349**, 842 (2015).

[26] D. J. Luitz, N. Laflorencie, and F. Alet, Extended slow dynamical regime close to the many-body localization transition, Phys. Rev. B **93**, 060201(R) (2016).

[27] F. Iemini, A. Russomanno, D. Rossini, A. Scardicchio, and R. Fazio, Signatures of many-body localization in the dynamics of two-site entanglement, Phys. Rev. B **94**, 214206 (2016).

[28] E. Levi, M. Heyl, I. Lesanovsky, and J. P. Garrahan, Robustness of Many-Body Localization in the Presence of Dissipation, Phys. Rev. Lett. **116**, 237203 (2016).

[29] J.-y. Choi, S. Hild, J. Zeiher, P. Schauß, A. Rubio-Abadal, T. Yefsah, V. Khemani, D. A. Huse, I. Bloch, and C. Gross, Exploring the many-body localization transition in two dimensions, Science **352**, 1547 (2016).

[30] H. P. Lüschen, P. Bordia, S. S. Hodgman, M. Schreiber, S. Sarkar, A. J. Daley, M. H. Fischer, E. Altman, I. Bloch, and U. Schneider, Signatures of Many-Body Localization in a Controlled Open Quantum System, Phys. Rev. X **7**, 011034 (2017).

[31] R. Singh, J. H. Bardarson, and F. Pollmann, Signatures of the many-body localization transition in the dynamics of entanglement and bipartite fluctuations, New J. Phys. **18**, 023046 (2016).

[32] P. Sierant, D. Delande, and J. Zakrzewski, Many-body localization due to random interactions, Phys. Rev. A **95**, 021601(R) (2017).

[33] J. H. Bardarson, F. Pollmann, and J. E. Moore, Unbounded Growth of Entanglement in Models of Many-Body Localization, Phys. Rev. Lett. **109**, 017202 (2012).

[34] L. Herviou, J. H. Bardarson, and N. Regnault, Many-body localization in a fragmented Hilbert space, Phys. Rev. B **103**, 134207 (2021).

[35] M. Serbyn, Z. Papić, and D. A. Abanin, Universal Slow Growth of Entanglement in Interacting Strongly Disordered Systems, Phys. Rev. Lett. **110**, 260601 (2013).

[36] J. A. Kjäll, J. H. Bardarson, and F. Pollmann, Many-Body Localization in a Disordered Quantum Ising Chain, Phys. Rev. Lett. **113**, 107204 (2014).

[37] S. Bera and A. Lakshminarayan, Local entanglement structure across a many-body localization transition, Phys. Rev. B **93**, 134204 (2016).

[38] G. De Tomasi, S. Bera, J. H. Bardarson, and F. Pollmann, Quantum Mutual Information as a Probe for Many-Body Localization, Phys. Rev. Lett. **118**, 016804 (2017).

[39] V. Oganesyan and D. A. Huse, Localization of interacting fermions at high temperature, Phys. Rev. B **75**, 155111 (2007).

[40] P. Ponte, A. Chandran, Z. Papić, and D. A. Abanin, Periodically driven ergodic and many-body localized quantum systems, Ann. Phys. (Amsterdam, Neth.) **353**, 196 (2015).

[41] B. De, P. Sierant, and J. Zakrzewski, On intermediate statistics across many-body localization transition, J. Phys. A: Math. Theor. **55**, 014001 (2022).

[42] J. Gray, S. Bose, and A. Bayat, Many-body localization transition: Schmidt gap, entanglement length, and scaling, Phys. Rev. B **97**, 201105(R) (2018).

[43] M. Gong, G. D. de Moraes Neto, C. Zha, Y. Wu, H. Rong, Y. Ye, S. Li, Q. Zhu, S. Wang, Y. Zhao, F. Liang, J. Lin, Y. Xu, C.-Z. Peng, H. Deng, A. Bayat, X. Zhu, and J.-W. Pan, Experimental characterization of the quantum many-body localization transition, Phys. Rev. Research **3**, 033043 (2021).

[44] P. Bordia, H. P. Lüschen, S. S. Hodgman, M. Schreiber, I. Bloch, and U. Schneider, Coupling Identical One-Dimensional Many-Body Localized Systems, Phys. Rev. Lett. **116**, 140401 (2016).

[45] M. J. Gullans and D. A. Huse, Dynamical Purification Phase Transition Induced by Quantum Measurements, Phys. Rev. X **10**, 041020 (2020).

[46] T. K. Kvorning, L. Herviou, and J. H. Bardarson, Time-evolution of local information: thermalization dynamics of local observables, arXiv:2105.11206.

[47] A. Nico-Katz, A. Bayat, and S. Bose, Information-theoretic memory scaling in the many-body localization transition, Phys. Rev. B **105**, 205133 (2022).

[48] P. Roushan, C. Neill, J. Tangpanitanon, V. M. Bastidas, A. Megrant, R. Barends, Y. Chen, Z. Chen, B. Chiaro, A. Dunsworth, A. Fowler, B. Foxen, M. Giustina, E. Jeffrey, J. Kelly, E. Lucero, J. Mutus, M. Neeley, C. Quintana, D. Sank *et al.*, Spectroscopic signatures of localization with interacting photons in superconducting qubits, Science **358**, 1175 (2017).

[49] K. Xu, J. J. Chen, Y. Zeng, Y. R. Zhang, C. Song, W. Liu, Q. Guo, P. Zhang, D. Xu, H. Deng, K. Huang, H. Wang, X. Zhu, D. Zheng, and H. Fan, Emulating Many-Body Localization with a Superconducting Quantum Processor, Phys. Rev. Lett. **120**, 050507 (2018).

[50] C. Zha, V. M. Bastidas, M. Gong, Y. Wu, H. Rong, R. Yang, Y. Ye, S. Li, Q. Zhu, S. Wang, Y. Zhao, F. Liang, J. Lin, Y. Xu, C.-Z. Peng, J. Schmiedmayer, K. Nemoto, H. Deng, W. J. Munro, X. Zhu *et al.*, Ergodic-Localized Junctions in a Periodically Driven Spin Chain, Phys. Rev. Lett. **125**, 170503 (2020).

[51] Q. Guo, C. Cheng, H. Li, S. Xu, P. Zhang, Z. Wang, C. Song, W. Liu, W. Ren, H. Dong, R. Mondaini, and H. Wang, Stark Many-Body Localization on a Superconducting Quantum Processor, Phys. Rev. Lett. **127**, 240502 (2021).

[52] Q. Guo, C. Cheng, Z.-H. Sun, Z. Song, H. Li, Z. Wang, W. Ren, H. Dong, D. Zheng, Y.-R. Zhang *et al.*, Observation of energy-resolved many-body localization, Nat. Phys. **17**, 234 (2021).

[53] A. B. Harris, Effect of random defects on the critical behaviour of Ising models, J. Phys. C: Solid State Phys. **7**, 1671 (1974).

[54] J. T. Chayes, L. Chayes, D. S. Fisher, and T. Spencer, Finite-Size Scaling and Correlation Lengths for Disordered Systems, Phys. Rev. Lett. **57**, 2999 (1986).

[55] A. Chandran, C. R. Laumann, and V. Oganesyan, Finite size scaling bounds on many-body localized phase transitions, arXiv:1509.04285.

[56] Z.-H. Sun, J. Cui, and H. Fan, Characterizing the many-body localization transition by the dynamics of diagonal entropy, Phys. Rev. Research **2**, 013163 (2020).

[57] R. Vosk, D. A. Huse, and E. Altman, Theory of the Many-Body Localization Transition in One-Dimensional Systems, Phys. Rev. X **5**, 031032 (2015).

[58] P. T. Dumitrescu, R. Vasseur, and A. C. Potter, Scaling Theory of Entanglement at the Many-Body Localization Transition, Phys. Rev. Lett. **119**, 110604 (2017).

[59] A. Morningstar and D. A. Huse, Renormalization-group study of the many-body localization transition in one dimension, Phys. Rev. B **99**, 224205 (2019).

[60] J. Šuntajs, J. Bonča, T. Prosen, and L. Vidmar, Quantum chaos challenges many-body localization, Phys. Rev. E **102**, 062144 (2020).

[61] N. Laflorencie, G. Lemarié, and N. Macé, Chain breaking and Kosterlitz-Thouless scaling at the many-body localization transition in the random-field Heisenberg spin chain, Phys. Rev. Research **2**, 042033(R) (2020).

[62] A. S. Holevo, Bounds for the quantity of information transmitted by a quantum communication channel, Probl. Inf. Transm. **9**, 177 (1973).

[63] W. Roga, M. Fannes, and K. Zyczkowski, Universal Bounds for the Holevo Quantity, Coherent Information, and the Jensen-Shannon Divergence, Phys. Rev. Lett. **105**, 040505 (2010).

[64] M. A. Nielsen and I. L. Chuang, *Quantum Computation and Quantum Information: 10th Anniversary Edition*, 10th ed. (Cambridge University, Cambridge, England, 2011).

[65] This is true given our fixed probability distribution p_k, the Holevo quantity in practice is maximized over this distribution.

[66] J. Gray, quimb: A python library for quantum information and many-body calculations, J. Open Source Software **3**, 819 (2018).

[67] A. W. Sandvik, Computational studies of quantum spin systems, AIP Conf. Proc. **1297**, 135 (2010).

[68] L. D'Alessio and A. Polkovnikov, Many-body energy localization transition in periodically driven systems, Ann. Phys. (Amsterdam, Neth.) **333**, 19 (2013).